The Journal of Infectious Diseases

SUPPLEMENT ARTICLE

Fully Human Immunoglobulin G From Transchromosomic Bovines Treats Nonhuman Primates Infected With Ebola Virus Makona Isolate

Thomas Luke,[1] Richard S. Bennett,[2] Dawn M. Gerhardt,[2] Tracey Burdette,[2] Elena Postnikova,[2] Steven Mazur,[2] Anna N. Honko,[2,a] Nicholas Oberlander,[2] Russell Byrum,[2] Dan Ragland,[2] Marisa St. Claire,[2] Krisztina B. Janosko,[2] Gale Smith,[3] Gregory Glenn,[3] Jay Hooper,[4] John Dye,[4] Subhamoy Pal,[1] Kimberly A. Bishop-Lilly,[5] Theron Hamilton,[5] Kenneth Frey,[5] Laura Bollinger,[2] Jiro Wada,[2] Hua Wu,[6] Jin-an Jiao,[6] Gene G. Olinger,[2,b] Bronwyn Gunn,[8] Galit Alter,[8] Surender Khurana,[9] Lisa E. Hensley,[2] Eddie Sullivan,[6] and Peter B. Jahrling[2,7]

[1]Viral and Rickettsial Diseases Department, Naval Medical Research Center, The Henry Jackson Foundation for the Advancement of Military Medicine, Silver Spring, Maryland; [2]Integrated Research Facility at Fort Detrick, National Institute of Allergy and Infectious Diseases, National Institutes of Health, Frederick, Maryland; [3]Novavax, Inc., Gaithersburg, Maryland; [4]Virology Division, United States Army Medical Research Institute of Infectious Diseases, Fort Detrick, Maryland; [5]Biological Defense Research Directorate, Naval Medical Research Center, Ft. Detrick, Maryland; [6]SAB Biotherapeutics Inc., Sioux Falls, South Dakota; [7]Emerging Viral Pathogens Section, National Institute of Allergy and Infectious Diseases, National Institutes of Health, Frederick, Maryland; [8]Ragon Institute of Massachusetts General Hospital, Massachusetts Institute of Technology, and Harvard, Boston; [9]Division of Viral Products, Center for Biologics Evaluation and Research, US Food and Drug Administration, Silver Spring, Maryland

Transchromosomic bovines (Tc-bovines) adaptively produce fully human polyclonal immunoglobulin (Ig)G antibodies after exposure to immunogenic antigen(s). The National Interagency Confederation for Biological Research and collaborators rapidly produced and then evaluated anti-Ebola virus IgG immunoglobulins (collectively termed SAB-139) purified from Tc-bovine plasma after sequential hyperimmunization with an Ebola virus Makona isolate glycoprotein nanoparticle vaccine. SAB-139 was characterized by several in vitro production, research, and clinical level assays using wild-type Makona-C05 or recombinant virus/antigens from different Ebola virus variants. SAB-139 potently activates natural killer cells, monocytes, and peripheral blood mononuclear cells and has high-binding avidity demonstrated by surface plasmon resonance. SAB-139 has similar concentrations of galactose-α-1,3-galactose carbohydrates compared with human-derived intravenous Ig, and the IgG1 subclass antibody is predominant. All rhesus macaques infected with Ebola virus/H.sapiens-tc/GIN/2014/Makona-C05 and treated with sufficient SAB-139 at 1 day (n = 6) or 3 days (n = 6) postinfection survived versus 0% of controls. This study demonstrates that Tc-bovines can produce pathogen-specific human Ig to prevent and/or treat patients when an emerging infectious disease either threatens to or becomes an epidemic.

Keywords. Ebola; therapeutic; countermeasure; rhesus; bovine.

Several passive immunotherapeutics are under development to treat emerging infectious diseases and filoviruses [1–6]. However, traditional human-derived and heterologous animal-derived polyclonal immunoglobulins (Igs) and monoclonal antibodies can have lengthy development and/or clinical safety issues [1, 7, 8]. To address these shortcomings, genetically modified transchromosomic bovines (Tc-bovines) were developed that adaptively produce fully human polyclonal antibodies after exposure to environmental or vaccine antigens [9–12]. After hyperimmunization, Tc-bovine fully human IgG (Tc-hIgG) can be rapidly produced from their plasma [13–16]. Tc-bovines, depending upon age and size, produce 150 to 600 grams of purified Tc-hIgG per month. Experimental high-titer Tc-hIgGs were produced against several pathogens and demonstrated efficacy in animal models. In a recent study, 2 Tc-hIgG Investigational New Drug applications (ClinicalTrials.gov nos. NCT02788188 and NCT02508584) were approved by the US Food and Drug Administration for Middle East respiratory syndrome coronavirus (MERS CoV) [17] and *Mycoplasma hominis* indications (termed SAB-301 and SAB-136, respectively). SAB-301 was safe and well tolerated in a completed phase I clinical trial with an average terminal IgG elimination half-life ($t_{1/2}$) of ~28 days (d) that is similar to human-derived intravenous Ig (IVIG) [18]. SAB-136 was safe and efficacious in a phase I clinical trial that treated a patient with severe immunodeficiency, hypogammaglobinemia, and chronic *M hominis* septic hip and polyarthritis. The patient received SAB-136 for 1 year, and the drug was well tolerated with no significant adverse events and displayed and his clinical parameters improved with decreased mycoplasma burden [19].

To respond to the Ebola virus (EBOV) disease epidemic in Africa, 3 federal laboratories of the National Interagency Confederation of Biological Research at Ft. Detrick, MD [20] led a consortium to sequentially produce and evaluate 3 purified

[a]Present Affiliation: DSI, Minneapolis, Minnesota.

[b]Present Affiliation: MRIGlobal-Global Health Surveillance and Diagnostics, Gaithersburg, Maryland.

Correspondence: E. Sullivan, PhD, 2301 E. 60th St N., Sioux Falls, SD 57104 (esullivan@sabbiotherapeutics.com).

The Journal of Infectious Diseases® 2018;218(S5):S636–48

DOI: 10.1093/infdis/jiy377

good manufacturing practices (GMP) anti-EBOV Tc-hIgGs (collectively termed SAB-139) derived from Tc-bovines hyperimmunized with a recombinant EBOV/Makona isolate glycoprotein (rGP) vaccine [21]. In a previous study, a bench-scale non-GMP lot of SAB-139 produced after the second vaccination of Tc-bovines protected 90% of mice when administered 24 hours (h) after infection with mouse-adapted EBOV [13]. In this study, we report SAB-139's characteristics and efficacy against EBOV infection in a series of in vitro and rhesus macaque experiments.

METHODS

Ethics Statement

All National Institute of Allergy and Infectious Diseases (NIAID) Integrated Research Facility (IRF) and SAB animal facilities and animal programs are accredited by the Association for Assessment and Accreditation of Laboratory Animal Care International. The study protocols were reviewed and approved by the SAB and NIAID IRF Institutional Animal Care and Use Committees in compliance with all applicable federal regulations governing the protection of animals and research.

Transchromosomic Bovine Production, Hyperimmunization, and Plasma Collection

Transchromosomic bovine production was previously described [9–12]. Two Tc-bovines were immunized intramuscularly (IM) with EBOV/Makona rGP (2014 Zaire variant; Novavax, Inc.) [21] formulated with SAB's proprietary adjuvant SAB-adj-1. The Tc-bovines were vaccinated 8 times (V1–V8) at 3- to 4-week (wk) intervals. The antigen dose was 2 mg per animal for first vaccination (V1)–V4 and 5 mg per animal for V5–V8. Plasma and serum samples were taken at various time points before and/or after each vaccination.

Before the V1, a volume of prevaccination plasma was collected from each study Tc-bovine for use as negative control Tc-hIgG. Up to 2.1% of body weight of hyperimmune plasma per animal per time point was collected from immunized Tc-bovines for anti-EBOV fully human polyclonal antibody production (on d 8, 11, and 14 postvaccination starting from V2 to V8). Plasma was collected using an automated plasmapheresis system (Autopheresis C Model 200; Baxter Healthcare) and stored frozen at –20°C until purifications were performed.

Purification of Fully Human Immunoglobulin G

Production of Tc-hIgG from Tc-bovine plasma was previously described [13].

Virus Source and Propagation

The EBOV/Mak-C05 isolate was Ebola virus/H.sapiens-tc/GIN/2014/EBOV/Mak-C05 (GenBank accession no. KP096420.1) [22]. The culture methods for the study virus stock (internal reference IRF0137) were previously described [23]. The virus stock was 98.9% 7U genotype (GenBank accession no. KX000400.1) determined by next-generation sequencing as previously described [24].

Pseudovirion Neutralization Assay

The pseudovirion neutralization assay (PsVNA) was performed as previously described [13, 25]. The assays were conducted using nonreplicating vesicular stomatitis virus without GP (VSVΔG). The GP was replaced by luciferase pseudotyped with EBOV Kikwit 1995 variant GP. The PsVNA-50% ($PsVNA_{50}$) titers for the samples were the average of 2 independent experiments.

Cells Used in Neutralization Assays

For fluorescence reduction neutralization assay-50% ($FRNA_{50}$) and plaque reduction neutralizing test-50% ($PRNT_{50}$), African green monkey kidney cells (VERO C1008 [E6]; CRL-1586, American Type Tissue Culture Collection [ATCC], Manassas, VA) were maintained in Dulbecco's modified Eagle's medium (DMEM) with high glucose and L-glutamine (catalog no. 12-604Q, Lonza, Walkersville, MD) containing 10% heat-inactivated fetal bovine serum (catalog no. F2442, MilliporeSigma Life Science Research, Danvers, MA). The cells were seeded 1 d before use at 4×10^4 cells/well in 96-well plates (catalog no. 655948, Greiner Bio-One North America, Monroe, NC) and 1×10^6 cells/well in 6-well plates (catalog no. 3506, Corning, Corning, NY), respectively, and incubated at 37°C with 5% CO_2.

Fluorescence Reduction Neutralizing Assay-50%

Samples from SAB-139 lots 1–3 were thawed and used immediately without heat inactivation. Test samples were serially diluted (1:2) over 10 dilutions in cell culture media without added fetal bovine serum. The EBOV Makona isolate was diluted and mixed 1:1 with the sample to achieve a final target titer of 40 000 plaque-forming units (PFU)/well. The virus/sample mixture was incubated at 37°C with 5% CO_2 for 1 h, transferred to a 96-well plate containing confluent Vero E6 cells, and incubated at 37°C with 5% CO_2 for 48 h. An anti-EBOV antibody (catalog no. 0315-001, IBT Bioservices, Rockville, MD) was included to confirm assay performance.

Plates were fixed with 2× buffered formalin (30 minutes [min] at room temperature) and with 10% buffered formalin overnight. Cells were permeabilized with Triton buffer (0.25% Triton X-100) in 1× phosphate-buffered saline (PBS) for 5 min at room temperature. The plates were then washed 3 times and blocked with 1.5% normal goat serum. The cells were stained with an anti-EBOV antibody (mouse anti-VP40 B-MD04-BD07-AE11; US Army Medical Research Institute of Infectious Diseases, Frederick, MD), washed, stained with a fluorescently labeled secondary antibody (goat antimouse; catalog no. A11029, Life Technologies, Carlsbad, CA), and visualized by a High-Content Imaging System Operetta (PerkinElmer,

Waltham, MA). The $FRNA_{50}$ values were determined to be the dilution with a 50% reduction in virus-positive cells compared with wells only containing virus (no antibodies).

Plaque Reduction Neutralizing Test-50%

Plaque reduction neutralization test was performed as previously described [26], with the following exceptions. After incubation, 100 µL instead of 300 µL of virus/serum inoculum were added to duplicate wells of a 6-well plate containing 90%–100% confluent Vero E6 cells in 700 µL DMEM with 10% fetal bovine sera and 1% penicillin-streptomycin (catalog no. 15140122, Thermo Fisher Scientific).

Enzyme-Linked Immunosorbent Assay Titers

Enzyme-linked immunosorbent assay (ELISA) titers were determined using the human anti-EBOV antibodies against GP or nucleoprotein (NP) as previously described [26]. Assay results were considered valid if the sample duplicates had a coefficient of variance of <20% and the internal positive control had an optical density (OD) of >0.5 OD units.

Antibody-Mediated Monocyte Phagocytosis

Recombinant EBOV GP without the transmembrane protein (ΔTM) (catalog no. 0501-016, IBT Bioservices, Rockville, MD) was biotinylated and conjugated to Neutravidin™-coated yellow-green fluorescent 1 µm beads (catalog no. F-8776, Thermo Scientific, Waltham, MA). SAB-139, Tc-bovine sera, and/or purified IgG subclasses, irrelevant Tc-hIgG, KZ52, or c13C6 (250 µg/mL) were incubated for 2 h at 37°C. Human monocytic cells (THP-1; ATCC) were added at a concentration of 2.5×10^4 cells/well and incubated for approximately 18 h at 37°C. Cells were fixed and analyzed by flow cytometry, and a phagocytic score was determined using the percentage of fluorescein isothiocyanate $(FITC)^+$ cells and the geometric mean fluorescent intensity ([gMFI] FITC) of the $FITC^+$ cells [(%$FITC^+$ cells × gMFI FITC)÷10 000].

Antibody-Mediated Neutrophil Phagocytosis

The EBOV GP-coupled Alexa488 beads were generated as described for antibody-mediated monocyte phagocytosis (ADMP) (see above). SAB-139, Tc-bovine sera, and/or purified IgG subclasses, irrelevant Tc-hIgG, KZ52, or c13C6 (250 µg/mL) were incubated with EBOV GP-coupled beads for 2 h at 37°C. Human neutrophils freshly isolated from peripheral blood were added at a concentration of 5.0×10^4 cells/well and incubated for 1 h at 37°C. Cells were stained for CD66b (BioLegend no. 305112), CD3 (catalog no. 557943, BD Biosciences, San Jose, CA), and CD14 (catalog no. 557831, BD Biosciences) and analyzed by flow cytometry on a BD LSR II flow cytometer (BD, Franklin Lakes, NJ). Neutrophils were defined as side scatter-A high $CD66b^+$, $CD14^-$, and $CD3^-$. A phagocytic score was determined using the percentage of $FITC^+$ cells and the gMFI of the $FITC^+$ cells.

Natural Killer Cell Activation and Degranulation

The EBOV-GPΔTM (3 µg/mL) was coated on a Maxisorp ELISA plate (Thermo Scientific). Plates were blocked with 5% bovine serum albumin before addition of 250 µg/mL Tc-hIgG for 2 h at 37°C. Human natural killer (NK) cells were enriched from peripheral blood mononuclear cells by negative selection with specific antibodies using RosetteSep (catalog no. 15065, STEMCELL Technologies, Cambridge, MA). The NK cells were added at 5×10^4 cells/well in the presence of brefeldin A (catalog no. B7651, Millipore Sigma), GolgiStop (catalog no. 554724, BD Biosciences), and anti-CD107a (catalog no. 555802, BD Biosciences) and incubated for 5 h at 37°C. Natural killer cells were stained for surface markers of NK cells (CD3, CD56, CD16; BD Biosciences) and then intracellularly stained for interferon (IFN)-γ and macrophage inflammatory protein (MIP)-1β (BD Biosciences). Cells were analyzed by flow cytometry on a BD LSR II flow cytometer (BD Biosciences), and data were analyzed using FlowJo software (FlowJo, Ashland, OR).

Determination of Ebola Virus Glycoprotein-Specific Immunoglobulin G Subclasses Using Microspheres

The EBOV rGP (IBT Bioservices) was coupled to fluorescent microspheres (Luminex, Austin, TX) by carbodiimide cross-linker chemistry using *N*-hydroxysulfosucciminimide and 1-(3-dimethylaminopropyl)-3-ethylcarbodiimide (Thermo Fisher Scientific). Coupled beads were incubated with antibody samples (0.25 mg/mL) with shaking at 500 revolutions per min overnight at 4°C, and unbound antibodies were removed by washing 3 times with PBS + 0.05% Tween 20. Specific subclasses were detected using 1.3 µg/mL phycoerythrin-conjugated secondary antibodies specific for human IgG, IgG1, IgG2, IgG3, and IgG4 (Southern Biotech, Birmingham, AL) for 2 h at room temperature with shaking. The mean fluorescent intensity was determined through acquisition of a minimum of 50 beads on BioPlex 3D Suspension Array System (Bio-Rad, Hercules, CA).

Human Immunoglobulin G (IgG) Subclass Proportion in Transchromosomic Human IgG by Enzyme-Linked Immunosorbent Assay

Proportions of human IgG1, IgG2, IgG3, and IgG4 in SAB-139 (V3–V4) and SAB-139 (V6–V8) were determined using IgG subclass ELISAs as previously described [1].

Real-Time Antibody Kinetics by Surface Plasmon Resonance

Steady-state equilibrium binding of purified Tc-bovine IgG was monitored using a ProteOn surface plasmon resonance (SPR) system (Bio-Rad) as previously described [13] with the following exceptions. Samples of 300 µL instead of 200 µL freshly prepared IgG preparations were evaluated. Parallel antibody dissociation curves for 100 µg/mL, 33 µg/mL, and 10 µg/mL for each postvaccination IgG sample were established as previously described [13].

Assessment of Galactose-α-1,3-Galactose in Transchromosomic Human Immunoglobulin G by Enzyme-Linked Immunosorbent Assay

The presence of galactose-α-1,3-galactose (α-gal) was assessed in Tc-hIgG by an ELISA method using a murine anti-α-1,3-galactose-specific monoclonal antibody (M86; catalog no. ALX-801-090-1, Enzo Life Sciences, Farmingdale, NY) that specifically binds to α-gal residues. Test samples, controls, and blanks coated the wells of a 96-well plate, and 5% nonfat dry milk was used as a blocking agent. After washing with PBS containing 0.05% Tween 20, murine anti-α-1,3-galactose monoclonal antibody (M86) was added to each well at a 1:100 dilution per manufacturer's instructions. Anti-mouse IgM horseradish peroxidase (HRP) was diluted at 1:10 000 and then used as a detection antibody. Bound HRP activity was detected by adding 3,3′,5,5′-tetramethylbenzidine substrate (catalog no. 50-76, KPL). The OD values at 450 nm were measured by an automated Microplate Reader (Model PowerWaveXS; BioTek Instrument Inc.). Blank and negative controls had an OD 450 value of <0.2 in this ELISA method. Test samples and controls include the following: Tc-hIgG (SAB Biotherapeutics Inc., Sioux Falls, SD); antithymocyte globulin (ATG) equine (Pfizer, New York, NY); and ATG rabbit (Thymoglobulin; Sanofi US, Bridgewater, NJ). Human IVIG (Flebogamma 5% dual inactivation plus nanofiltration; Grifols) was used as a negative control, and cetuximab (Erbitux; Bristol-Myers Squibb, New York, NY) was used as a positive control. Cetuximab (a gift from Dr. John Lee, Sanford Research, Sioux Falls, SD) is known to contain α-gal.

Infection, Treatment, and Observation of Study Animals

Prescreened, quarantined, healthy rhesus macaques (*Macaca mulatta*) were randomized to groups, and age and weight (*t* test) and sex (Fisher's exact test) group means were not significantly different before infection. Macaques received a target dose of 1000 PFU of EBOV/Mak-C05 isolate IM in the upper arm on d 0 (experiments 1, 2, 3). Survivors from experiment 2 were rechallenged at d 77. The target dose of SAB-139 or irrelevant Tc-hIgG was delivered as a diluted saline IV infusion of 2 mL/kg at a rate of 2 mL/min. Blood and cerebrospinal fluid (CSF) were collected periodically until end of study (EOS) to assess blood chemistry parameters and/or for EBOV/Mak-C05 quantification, but collection differed by treatment group and time of collection (Figure 2) [23, 27]. Euthanasia criteria were established a priori. All staff collecting samples or clinical data, investigators, or veterinarians responsible for euthanasia decisions were blinded to nonhuman primate (NHP) group assignment.

Experiment 1 Using SAB-139/V3–V4

Fourteen NHPs (11 males and 3 females, 2 to 5 years of age) were randomLy assigned to 3 groups: an early-intervention (EI) group (N = 6), an irrelevant Tc-hIgG control group (N = 6), or an infection-control group (normal saline) (N = 2). The target infection dose was 1000 PFU (2121 PFU actual) of EBOV/Mak-C05 isolate given IM on d 0. On d 1, 3, 6, and 12 postinfection, the NHPs were scheduled to receive to 57 mg/kg of SAB-139/V3–V4, irrelevant Tc-hIgG, or equivalent volume normal saline (Figure 2A). The target dose and administration schedule were based upon neutralization titers, the opinion of the investigators, and the time constraints needed to infuse all NHPs under sedation in a biosafety level 4 (BSL4) setting.

Experiment 2 Using SAB-139/V6–V8

Fourteen NHPs (8 males and 6 females, 2 to 15 years of age) were randomly assigned to 3 groups: an EI group (N = 6), a delayed-intervention (DI) group (N = 6), or an irrelevant Tc-hIgG control group (N = 2). The target infection dose was 1000 PFU (2300 PFU actual dose) of EBOV/Mak-C05 isolate given IM on d 0. On d 1, 4, 7, and 10 postinfection of the EI and irrelevant Tc-hIgG groups and on d 3, 6, 9, and 12 postinfection of the DI group, the NHPs were scheduled to receive 150 mg/kg for the first 3 infusions and 125 mg/kg for the fourth infusion of SAB-139/V6–V8 or irrelevant Tc-hIgG (Figure 2B). The target dose and administration schedule were based upon results of experiment 1 and the ability to deliver a maximum infused dose within the time constraints needed to infuse all NHPs under sedation in a BSL4 setting.

Experiment 2: Assessment of Adaptive Immune Response After Back-Challenge. Ten NHP survivors from the EI (n = 6) and DI (n = 4) groups were back-challenged with a target dose of 1000 PFU (615 PFU actual dose) of EBOV/Mak-C05 isolate given IM on d 77 after initial challenge to assess adaptive immunity (Figure 2B).

Experiment 3 Using SAB-139/V6–V8

Twelve NHPs (6 males and 6 females, 3 to 7 years of age) were randomly assigned to 3 groups: a late-intervention (LI) group (N = 6), an irrelevant Tc-hIgG control group (N = 2), or a saline control group (N = 4). The target infection dose was 1000 PFU (2120 PFU actual dose) of EBOV/Mak-C05 isolate given IM on d 0. On d 5, 7, 9, and 11–14 postinfection, the NHPs were scheduled to receive 4 doses of 150 mg/kg SAB-139/V6–V8, irrelevant Tc-hIgG, or equivalent volume normal saline (Figure 2C). The target dose and administration schedule were based upon results of experiment 2. The administration of the fourth dose could vary depending upon the clinical status of the animal.

Blood Chemistries

Nonhuman primate serum chemistries were performed as previously described [23, 28].

Quantitative Real-Time Reverse-Transcription Polymerase Chain Reaction

Quantitative polymerase chain reaction (PCR) was performed as previously described [23]. Plasma virus load was measured using BEI Resources Critical Reagents Program (CRP) EZ1 quantitative reverse-transcription-PCR kit assay in accordance

with manufacturer's instructions and reported as gene equivalents (GE) per µL of sample.

Escape Mutant Analysis

The EBOV PCR$^+$ samples from NHPs in experiments 1 and 2 were analyzed for escape mutants resistant to SAB-139 by deep sequence analysis as previously described [29, 30]. Frozen, TRIzol-treated tissue homogenates and cell-free fluid samples were processed for extraction of total RNA using Directzol (Zymo Research, Irvine, CA) according to manufacturer's protocol. An on-column DNase digestion step was included. RNA was eluted in a volume of 20 µL. RNA integrity and purity were assayed using an RNA 6000 Pico chip on the Agilent Bioanalyzer (Agilent Technologies, Santa Clara, CA). RNA mass was determined by fluorescent detection using Qubit Broad Range RNA kit (Life Technologies). All RNA samples were stored at −80°C until use. Illumina RNA Access libraries (Illumina, San Diego, CA) were prepared for Illumina probe-capture library construction using an input of 200 ng of total RNA and following manufacturer's protocol. First and second hybridizations were performed on groups of 4 individual libraries using a custom set of 80-mer probes specific for EBOV. Probes were tiled across the genomes of 8 representative members of the filovirus family (Supplementary Table 10). All representative genomes were complete genomes. Probed libraries were quality checked using a deoxyribonucleic acid (DNA) 1000 chip on an Agilent Bioanalyzer. Libraries were pooled into groups of 4 before sequencing on an Illumina MiSeq using v3 chemistry (2 × 300 base pairs; paired-end).

Statistical Analysis

Effector cell functions of SAB-139 and Tc-bovine sera were evaluated by using the Spearman correlation coefficient and JMP Pro 12 software (SAS Institute, Cary, NC). R values were calculated using JMP, and a heat map was generated using Gene-E software (Broad Institute, Cambridge, MA). A *t* test and Fisher's exact test determined the similarity of randomized groups by age and weight (*t* test) and sex (Fisher's exact test) using R open software (R Foundation, Vienna, Austria) [31] and Spotfire S+ version 8.2.0 (Tibco Software, Palo Alto, CA). Descriptive data, tables, and figures are presented for all other results.

RESULTS

In Vitro Antibody Neutralization and Quantification Assays of SAB-139

Three sequential GMP lots of SAB-139 were produced from the postvaccination plasma of 2 Tc-bovines: lot 1 was produced from the plasma after the third and fourth vaccinations (SAB-139/V3–V4), and Lots 2 and 3 were produced from plasma after the sixth through eighth vaccinations (SAB-139/V6–V8). The SAB-139 lots were tested for antibody neutralization and/or titers to EBOV GP and/or NP per mg of each lot by $PsVNA_{50}$ (Kikwit-95 GP recombinant virus), $FRNA_{50}$ (Makona C05 wild-type virus), $PRNT_{50}$ (Makona C05 wild-type virus), and an ELISA (Kikwit-95 recombinant GP/NP proteins) as used by the different collaborators (Table 1). The $PsVNA_{50}$ titers for individual vaccination time points (V2, V3–V4, V6–V8) of Tc-bovine nos. 2314 and 2316 were published previously [13]. The $PsVNA_{50}$ and $PRNT_{50}$ neutralization titers of SAB-139/V3–V4 (Lot 1) compared with SAB-139/V6–V8 (Lot 2 and 3) were approximately 2.6 or 4.1 times and 17 or 26 times less, respectively. In contrast, the $FRNA_{50}$ and ELISA rGP (ELISA units [EU]/mg) titers had <2 times difference between all SAB-139 lots. The ELISA rNP titers were not detectable in any lot of SAB-139 (Table 1).

Ebola Virus-Specific Transchromosomic Bovine Serum and SAB-139 Recruit Innate Immune Effector Cell Functions

Postvaccination Tc-bovine sera (V1–V8), SAB-139/V3–V4 and SAB-139/V6–V8 (Lot 3), irrelevant Tc-hIgG (internal control), the anti-EBOV monoclonal antibodies c13C6 and KZ52 [32, 33] (positive controls), and saline (negative control) were evaluated for the ability to induce phagocytosis by monocytes or neutrophils and degranulation of NK cells in vitro by culturing with fluorescent beads [34] coated with EBOV rGP (Kikwit-95). Irrelevant Tc-hIgG did not induce human monocytes or neutrophils for ADMP, antibody-mediated neutrophil phagocytosis (ADNP) or activate NK cells (as measured by expression of CD107a and secretion of IFN-γ and MIP-1β proteins after degranulation) above the background levels established with normal saline (Figure 1A–C). The Tc-bovine sera antibodies (with all antibody classes) recruited ADMP activity above background after V2, yet ADMP activity gradually decreased after

Table 1. SAB-139 Titers Against Homologous and Heterologous Ebola Virus Variants From In Vitro Assays

				ELISA EU/mg[a]	
SAB-139 After Vaccinations (Lot no.)	$PsVNA_{50}$/mg[a]	$FRNA_{50}$/mg[a]	$PRNT_{50}$/mg[a]	GP	NP
V3–V4 (Lot 1)	1420	64	16	4056	<LOQ
V6–V8 (Lot 2)	3646	67	270	9008	<LOQ
V6–V8 (Lot 3)	5875	105	422	5480	<LOQ

Abbreviations: ELISA, enzyme-linked immunosorbent assay; EU, ELISA units; $FRNT_{50}$, fluorescent reduction neutralization assay 50%; GP, glycoprotein; LOQ, limit of quantification; NP, nucleoprotein; $PRNT_{50}$, plaque reduction neutralization test-50%; $PsVNA_{50}$, pseudovirion neutralization assay-50%.

[a]The PsVNA and ELISA used EBOV Kikwit 1995 isolate pseudovirions or recombinant GP, respectively, whereas the FRNA and PRNT used EBOV Makona C05 isolate.

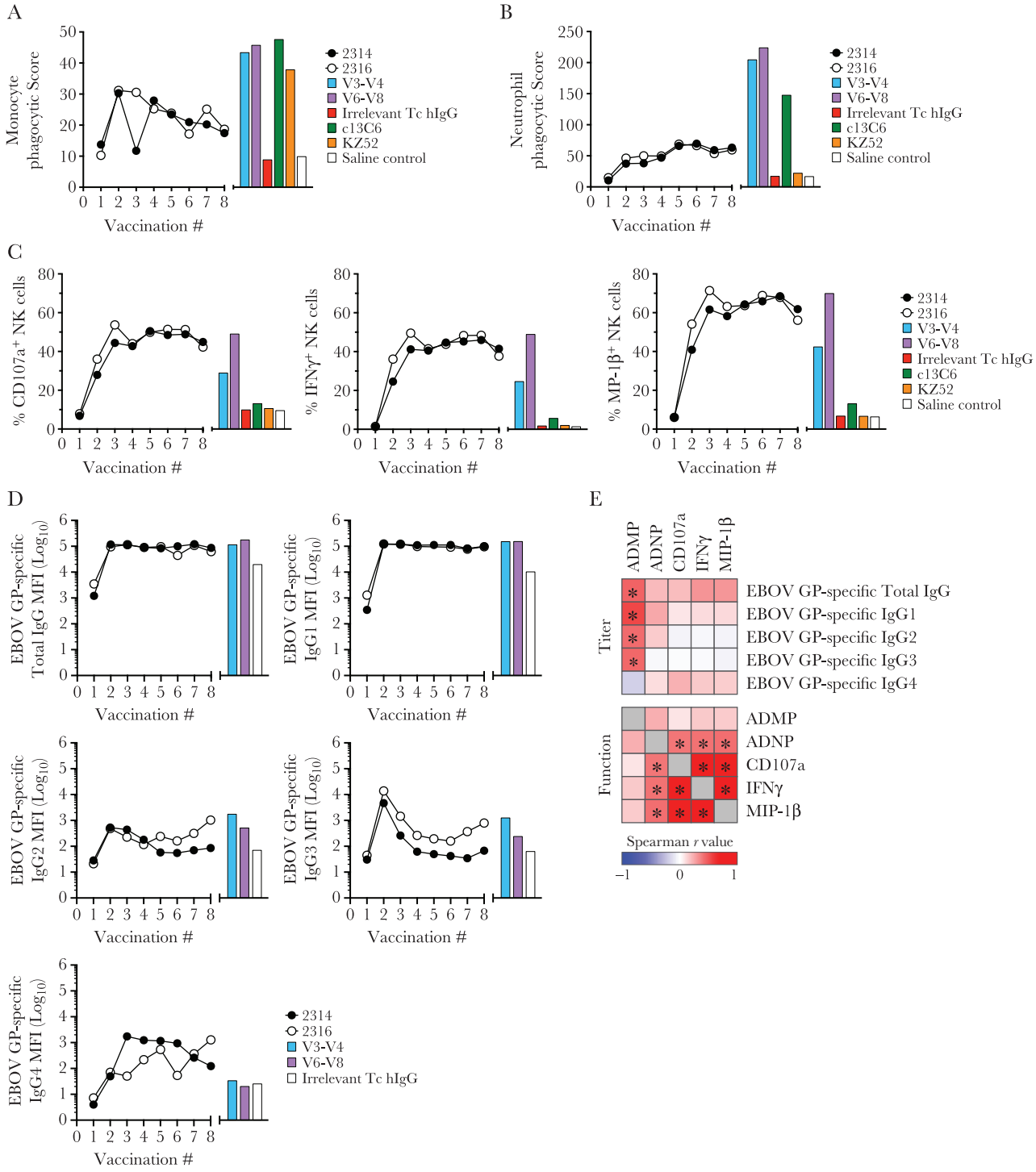

Figure 1. Ebola virus (EBOV)-specific transchromosomic bovine (Tc-bovine)-derived human immunoglobulin G (hIgG) potently recruits multiple innate immune effector functions. (A and B) Induction of antibody-mediated monocyte phagocytosis (ADMP) (A) or antibody-mediated neutrophil phagocytosis (ADNP) (B) using antibodies from SAB-139/V3–V4 (blue), SAB-139/V6–V8 (purple), sera from Tc-bovines (2314 [black squares] and 2316 [white circles]), anti-EBOV monoclonal antibodies c13C6 (green) and KZ52 (orange), no antibody control (white), and irrelevant Tc IgG control (red). Uptake of EBOV glycoprotein (GP) onto coated fluorescein isothiocyanate (FITC) beads was determined by flow cytometry. A phagocytic score was determined using the percentage of FITC$^+$ cells and the mean fluorescent intensity (MFI) of the FITC$^+$ cells. The average phagocytic score of 2 replicates is shown. (C) The percentage of natural killer (NK) cells expressing CD107a protein and production of the cytokine, interferon (IFN)-γ, and the chemokine macrophage inflammatory protein (MIP)-1b was determined by flow cytometry (average of 2 replicates). (D) EBOV-specific IgG subclass MFI was determined via Luminex EBOV GP-coupled beads followed by detection with a subclass-specific secondary antibody (average of 2 replicates). (E) Correlation analyses using Spearman correlation coefficients between ADMP, ADNP, CD107a, IFNγ, MIP-1β, and EBOV GP-specific subclass titers (total IgG, IgG1–4) indicated a significant correlation between indicated function and/or titer, as marked by an asterisk. The r_s values are represented by a heat map (range, –1 to 1).

each subsequent vaccination (V3–V8) (Figure 1A). In contrast, Tc-bovine serum antibodies recruited ADNP activity above background after V2, but ADNP gradually increased after each subsequent vaccination (V3–V8) (Figure 1B). Natural killer cell degranulation, as demonstrated by all 3 protein markers, was induced above background after V2, and the activity was sustained after each additional vaccination (Figure 1C). Although SAB-139/V3–V4 and SAB-139/V6–V8 had similar levels of ADMP and ADNP activity (Figure 1A and B), SAB-139/V6–V8 had higher induction of NK cell degranulation (Figure 1C). The c13C6 and KZ52 monoclonal antibodies induced ADMP, but only c13C6 antibody induced ADNP above background (Figure 1A and B). Neither anti-EBOV monoclonal antibodies c13C6 nor KZ52 induced NK cell degranulation above background (Figure 1C).

Immunoglobulin G Subclass Composition and Ebola Virus Glycoprotein-Specific Activity

SAB-139/V3–V4 (Lot 1) and SAB-139/V6–V8 (Lot 3) had a higher proportion of IgG1 compared with a human-derived IVIG (89%, 90%, and 61%, respectively) but had proportionally less IgG2, IgG3, and IgG4 (Table 2). The titers of EBOV GP-specific total IgG and the IgG1 subclass antibodies isolated from bovine sera, SAB-139/V3–V4 (Lot 1) and SAB-139/V6–V8 (Lot 3), were induced and sustained at high titers after V2 as determined by microsphere-based IgG methods [35] (Figure 1D). In contrast, the titers of EBOV GP-specific IgG2, IgG3, and IgG4 subclass antibodies isolated from bovine sera, SAB-139/V3–V4 and SAB-139/V6–V8, were 10 to 1000 times lower than for total IgG and the IgG1 subclass. Although these titers peaked at V2, they generally declined after additional vaccinations (Figure 1D).

Because the Fc fragment of different IgG-specific subclasses have varying affinity for cellular Fc receptors on effector cells [36–38], we next determined whether the induction of multiple Fc-mediated effector functions (eg, ADMP/ADNP, cytokine expression, activation of NK cells) correlated with an EBOV-GP IgG-specific subclass. To determine whether total IgG or an IgG subclass was associated with a specific function, Spearman coefficients were used to determine correlation. The ADMP activity had a significant positive association with total EBOV GP-specific IgG, IgG1, IgG2, and IgG3 but not IgG4, suggesting that ADMP activity is driven in part by antigen-specific antibody titer (Figure 1A and E). In contrast, neither ADNP nor NK cell degranulation/activation strongly correlated with any subclass, suggesting that the extent of induction of these functions is not solely based on antibody titer. To determine whether the ability of antibodies to induce a given function is associated with induction of other functions, correlation analyses were performed. Induction of ADMP activity did not strongly correlate with any other function (r_s <0.5), yet ADNP activity and NK cell degranulation and activation displayed moderate-to-very strong positive correlations ($r_s \geq 0.5$) with each other (Figure 1B, C, and E).

Surface Plasmon Resonance Analysis of SAB-139/V3–V4 and SAB-139/V6–V8 to Ebola Virus Glycoproteins

Steady-state equilibrium SPR analysis was used to evaluate total anti-EBOV antibodies and avidity of SAB-139/V6–V8 (Lot 3) and SAB-139/V3–V4 (Lot 1) to a homologous EBOV 2014-Makona isolate and a heterologous 1976-Mayinga rGP isolate immobilized on a histidine-tagged protein gold sensor chip [13]. Both the total antibody binding and antibody affinity of SAB-139/V6–V8 and SAB-139/V3–V4 were higher against the rGP of the homologous EBOV-Makona isolate compared with that observed with the heterologous EBOV-Mayinga isolate. The maximum resonance unit values for total anti-GP binding antibodies for SAB-139/V6–V8 were ~1.5- and ~2.5-fold higher than the EBOV-Mayinga GP and EBOV-Makona isolates, respectively, compared with SAB-139/V3–V4 antibodies (Supplementary Figure 1SA). The avidity of SAB-139/V6–V8 antibodies, as measured by antibody off-rate constants, was approximately 5-fold higher for both the EBOV-Mayinga GP and EBOV-Makona isolates compared with SAB-139/V3–V4 antibodies (Supplementary Figure 1SB).

Assessment of Transchromosomic Human Immunoglobulin G for Galactose-α-1,3-Galactose Levels

The α-gal residues can cause anaphylaxis in humans [7, 39], and, therefore, its presence was assessed in Tc-hIgG using an ELISA method. The level of α-gal from Tc-hIgG was similar to human IVIG, anti-thymoglobulin equine and rabbit polyclonal antibodies, and controls (OD values approximately 0.1 when tested

Table 2. Immunoglobulin G Subclass Percentages From Various Antibody Sources

	IgG Subclass			
Antibody	IgG1 (%)	IgG2 (%)	IgG3 (%)	IgG4 (%)
Human IVIG[a]	61.09	35.39	2.75	0.77
SAB-139 (V3–V4)	88.62	11.36	<LOQ	0.02
SAB-139 (V6–V8)	90.20	9.78	<LOQ	0.02

Abbreviations: ELISA, enzyme-linked immunosorbent assay; IgG, immunoglobulin G; IVIG, intravenous immunoglobulin; LOQ, limit of quantification.

[a]Human-derived IVIG served as the positive control and was run on the same IgG subclass ELISA plates with the other antibodies.

at 100 μg/mL). However, the α-gal level from the monoclonal antibody cetuximab (OD value approximately 3.3 when tested at 100 μg/mL) was 30-fold higher (Supplementary Table 1S).

Enzyme-Linked Immunosorbent Assay for Ebola Virus Recombinant Glycoprotein and Ribonucleoprotein Antibodies Pre- and Postinfusion With SAB-139

To evaluate efficacy of SAB-139 in NHPs against EBOV challenge, 3 experiments were conducted (Figure 2). ELISA IgG antibody serum titers against rGP target (EU/mL) preinfusion were below the limit of quantification (<LOQ) for all NHPs in all experiments. The ELISA rGP titers from NHPs from experiment 1 receiving EI (infusions on d 1, 3, 6, and 12 postinfection) with SAB-139/V3–V4 were measured on d 3 postinfection (range, 4606–7042 EU/mL) and fell by d 10 postinfection (range, 795–2008 EU/mL) (Figure 3 and Supplementary Table 2S). The ELISA rGP titers for EI (infusions on d 1, 4, 7, and 10 postinfection) and delayed DI (infusion initiated on d 3, 6, 9, and 12 postinfection) from NHPs from experiment 2 infused with SAB-139/V6–V8 initially measured on d 6 and/or 7 postinfection (range, 50 279–121 903 EU/mL) progressively fell by d 70 postinfection (range, 708–9006 EU/mL) (Figure 3 and Supplementary Table 3S). The rNP titers from experiment 2 for EI and DI NHPs preinfusion ranged from <LOQ to 200, peaked on d 14 or 28 (range, 340–27 727 EU/mL), and fell by d 70 postinfection (range, <LOQ of 308 EU/mL) (Supplementary Table 4S). The ELISA rGP titers from NHPs receiving LI (4 infusions initiated on d 5, 7, 9, and 11–14 postinfection) with SAB-139/V6–V8 in experiment 3 were measured at necropsy (range, 1688–3628 EU/mL) (Figure 3 and Supplementary Table 5S).

Protective Efficacy of SAB-139 Against EBOV/Mak-C05 Isolate Infection in Primates

Experiment 1

Two of 6 NHPs (33%) in the EI group survived until EOS (d 29) (Figure 3). Both survivors (animals 13 and 14) were clinically symptomatic with sporadic viremia and had detectable EBOV RNA within the CSF at necropsy. Most nonsurvivors in the EI group developed viremia (d 6 postinfection) and blood chemistry abnormalities and died on d 8 through 12 postinfection accompanied by virus within CSF at necropsy. All animals in the irrelevant Tc-hIgG and saline control groups developed viremia by d 3 postinfection and blood chemistry abnormalities and died by d 8 postinfection. Virus was detected in the CSF of most animals at necropsy (Supplementary Table 6S).

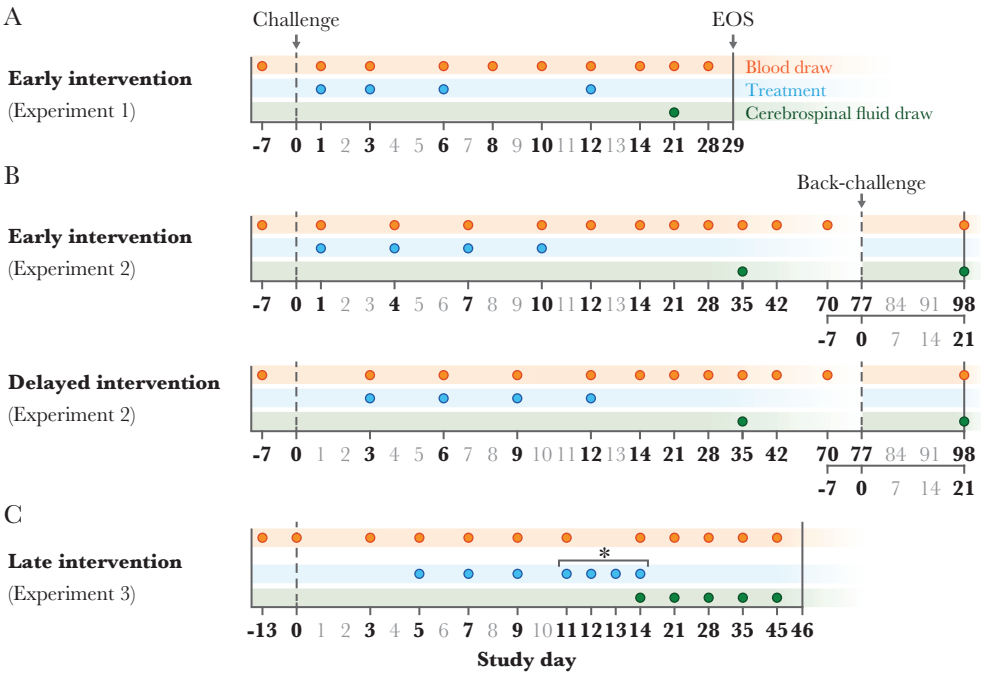

Figure 2. Study design. Three sequential Ebola virus (EBOV) challenge studies using Chinese-origin rhesus macaques were conducted to assess the postinfection efficacy of SAB-139 in early intervention ([EI] starting on 1 day [d] postinfection), delayed intervention ([DI] on 3 d postinfection) and late intervention ([LI] on 5 d postinfection). Collection of blood and cerebrospinal fluid samples was preplanned for each experiment, but collection differed by d based on group assignment and the experiment. (A) Experiment 1 evaluated 4 57 mg/kg intravenous (IV) doses of SAB-139/V3–V4 in an EI group (n = 6), an irrelevant transchromosomic human immunoglobulin G (Tc-hIgG) control group (n = 6), or a saline control group (n = 2). (B) Experiment 2 evaluated three 150-mg/kg doses then one 125-mg/kg IV dose of SAB-139/V6–V8 in EI (n = 6) and DI (n = 6) groups or an irrelevant Tc-hIgG in the control group (n = 2). Surviving animals were back-challenged at d 77 after initial challenge to assess the development of an adaptive immune response postinfection and treatment. (C) Experiment 3 evaluated three 150-mg/kg doses then one 125-mg/kg dose of SAB-139/V6–V8 in a LI group (n = 6), an irrelevant Tc-hIgG in a control group (n = 4), or saline in a negative control group (n = 2). The * indicates that the fourth administration could be administered on d 11, 12, 13, or 14 postinfection based upon clinical and laboratory criteria. Abbreviation: EOS, end of study.

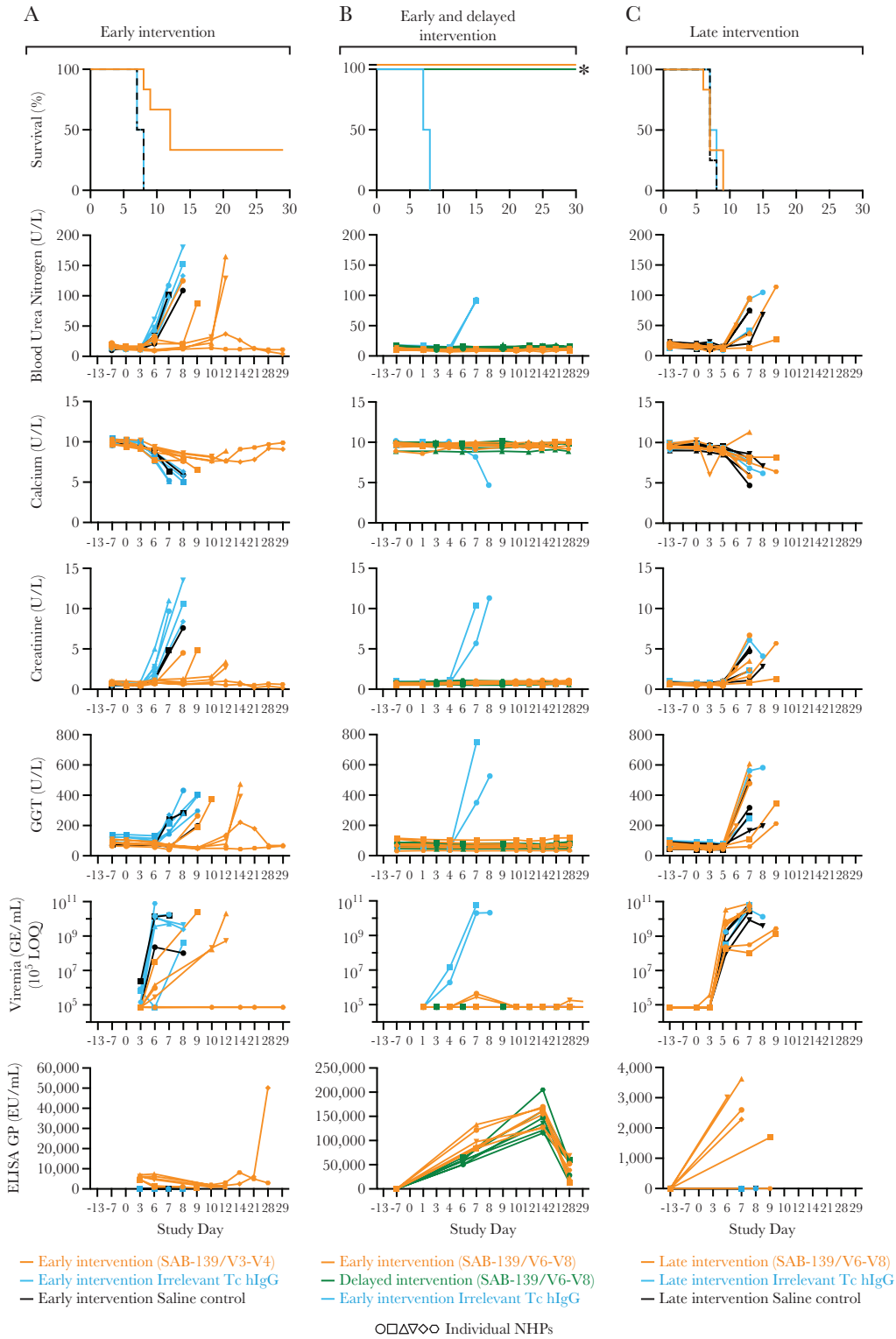

Figure 3. SAB-139 can reduce or eliminate morbidity and mortality in rhesus macaques. (A) Experiment 1: Of the early-intervention (EI) nonhuman primates (NHPs) receiving SAB-139/V3–V4 intravenous (IV), 33% survived (2 of 6) compared with 0% (0 of 6) after administration irrelevant transchromosomic human immunoglobulin G (Tc-hIgG) or normal saline (0 of 2) controls. Surviving animals had mild clinical signs but no detectable viremia (10^5 genome equivalents [GE]/mL limit of quantification [LOQ]). The NHPs had low anti-Ebola virus (EBOV) glycoprotein (GP) enzyme-linked immunosorbent assay (ELISA) titers after infusion (day [d] 3, 2908–7042 ELISA units [EU]/mL). One surviving NHP abruptly developed high anti-EBOV GP ELISA titers near end of study (EOS). (B) Experiment 2: Of EI and delayed intervention (DI) NHPs treated with SAB-139/V6–V8 IV, 100% survived (6 of 6 in both groups) compared with 0% of irrelevant Tc-hIgG controls (0 of 2). All SAB-treated NHPs were asymptomatic, but 2 EI animals had low sporadic viremia. All EI and DI NHPs had anti-EBOV GP ELISA titers after infusion that peaked at d 14 postinfection before falling at EOS. (C) Experiment 3: Of late intervention NHPs treated with SAB-139/V6–V8 IV, 0% survived (0 of 6) as did controls. All NHPs had viremia ranging from 10^8 to 10^{10} GE/mL at d 5 postinfection. All animals died before or on d 9 postinfection. All NHPs had a low anti-EBOV GP ELISA titer at necropsy (1688–3629 EU/mL). Abbreviation: GGT, gamma-glutamyl transferase.

Nonsurvivor blood chemistries at necropsy were consistent with lethal EBOV disease [23, 27] (Figure 3A).

Experiment 2

All animals in the EI and DI groups survived (12 of 12) without clinical signs of EBOV infection or blood chemistry abnormalities at EOS (d 35). Serum or CSF from animals 3 and 6 of the EI group had viremia on d 7 (2.7 to 4.3 × 10^5 GE/mL) and 28 (1.8 × 10^5 GE/mL) postinfection. Both NHPs receiving irrelevant Tc-hIgG developed viremia on d 4 postinfection (1.9 × 10^6 or 1.4 × 10^7 GE/mL) and blood chemistry abnormalities and succumbed to disease on d 7 or 8 postinfection with viremia (5.7 × 10^{10} or 2.0 × 10^{10} GE/mL) (Supplementary Table 7S and Figure 3B). Nonsurvivor blood chemistries at necropsy were consistent with lethal EBOV disease [23, 27].

Assessment of Adaptive Immune Response After Back-Challenge

Early-intervention (n = 6) and DI (n = 4) NHPs in experiment 2 were back-challenged with a target dose of 1000 PFUs of EBOV (611 actual PFU) 77 d after initial infection. Five of 6 NHPs in the EI group succumbed to disease on d 6–10 after back-challenge (d 83–87 after initial challenge) (Figure 4). The surviving animal (no. 6) did not develop detectable viremia (Supplementary Table 8S). All NHPs (4 of 4) in the DI group survived back-challenge, and viremia was not detected (Supplementary Table 8S and Figure 4). Only 4 NHPs in the DI group were available for back-challenge because 2 of the animals were euthanized on d 59 for non-EBOV-related conditions. In these animals, chronic ulcerative dermatitis and persistent diarrhea developed 35 d postinfection and were negative for evidence of EBOV infection at necropsy. Nonsurvivor EBOV plasma and CSF concentrations at necropsy and blood chemistries were consistent with lethal EBOV disease [23, 27].

Experiment 3

NHPs in the LI, irrelevant Tc-hIgG, and normal saline groups became viremic, and all but 1 (LI group) died by d 7 postinfection (Figure 3C, Supplementary Table 9S). EBOV CSF concentrations at necropsy (Supplementary Table 9S) and blood chemistries (Figure 3C) in nonsurvivors were consistent with lethal EBOV disease [23, 27].

Histopathological Results From Nonsurviving Nonhuman Primates From All Experiments

All animals that succumbed in all experiments underwent necropsy. Findings included multifocal petechiae on the ventral body surface and enlarged axillary lymph nodes that corresponded with the arm in which the virus was inoculated. Gross manifestations on necropsy included hemorrhage in the adrenal glands and mucosal hemorrhages in the stomach and urinary bladder. Kidney lesions ranged from vascular congestion to tubular necrosis, hemorrhage, and hemoglobinuria. Hemorrhage and intravascular fibrin thrombi were noted in the testes. Lesions in the cerebral cortex included vascular congestion and intravascular fibrin thrombi. These findings are consistent with lesions previously found in NHPs with lethal EBOV infections [23, 27]. Follow-up studies to quantify virus and antigen load in NHP survivor and nonsurvivor brains, retinas, and other tissues treated should be conducted.

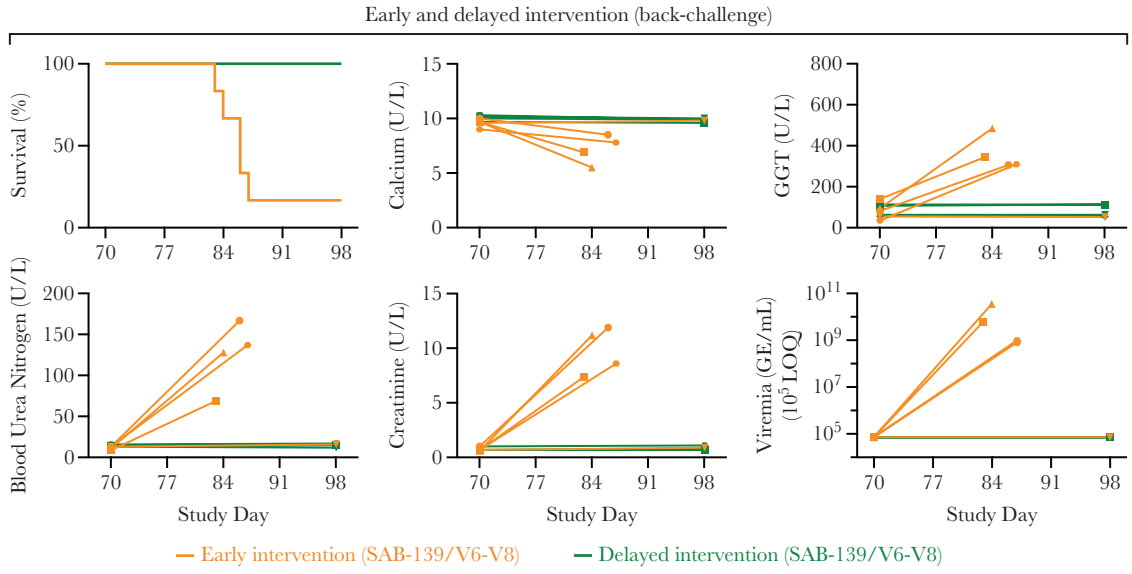

Figure 4. Back-challenge survival, blood chemistries, and viremia. Early intervention (EI) and delayed intervention (DI) nonhuman primates (NHPs) from experiment 2 were back-challenged with Ebola virus (target dose 1000 plaque-forming units) on day (d) 77 after initial exposure. Of the total NHPs in both groups (n = 10), 12.67% (1 of 6) of the EI group and 100% (4 of 4) of the DI group survived, respectively. Nonsurvivors had high viremia (8.3 × 10^8 to 3.6 × 10^{10} genome equivalents [GE]/mL). Survivors had no detectable viremia or changes in blood chemistries. Abbreviations: GGT, gamma-glutamyl transferase; LOQ, limit of quantification.

Escape Mutant Analysis

Deep sequencing of EBOV RNA isolates [29, 30] from PCR$^+$ serum and CSF samples from experiment 1 and 2 did not indicate resistance to SAB-139 due to a viral escape mutant.

DISCUSSION

The purpose of this effort was to rapidly develop an anti-EBOV immunotherapeutic from hyperimmunized Tc-bovines and evaluate its characteristics and efficacy in a number of in vitro and in vivo experiments. The in vitro assays to assess SAB-139 included those potentially useful in the clinical setting for patient management (ELISA assay), in the research setting (pseudovirus, PRNT/FRNA, SPR, or effector cell assays), in the GMP production setting for quality control/release specifications (IgG subclass and SPR assays), or in the regulatory setting to address potential patient-safety issues (α-gal assay) before clinical testing.

One consistent observation is that SAB-139/V6–V8 had a higher neutralization titer, total anti-EBOV antibodies, and avidity than SAB-139/V3–V4 in all assays regardless of whether the EBOV variant was homologous or heterologous. A likely explanation is that the affinity of Tc-bovine anti-EBOV IgG1 antibody clones continues to mature during the adaptive immune response after successive vaccinations that target both EBOV/Makona-specific epitopes and EBOV-conserved epitopes. This result likely indicates that Tc-hIgGs derived from plasma from later vaccinations are more potent than those derived from earlier vaccinations. Therefore, dosing of SAB-139 should be based upon the results of postproduction immunogenicity assays for each lot as correlated to future animal model and/or human efficacy observations.

We also show that Tc-bovine antibodies have similar levels of α-gal compared with a human-derived IVIG. The α-gal causes a human-immunologic barrier to xenotransplantation or anaphylaxis/hypersensitivity reactions in some humans after equine antivenom or cetuximab administration or red meat consumption, and SAB-139 should not cause α-gal-related reactions [7, 8, 39]. Results from the recently completed phase I clinical trial in healthy adults for SAB-301 (anti-MERS CoV) [18] indicated that it was well tolerated, but further studies in humans to determine safety and/or immunogenicity will be needed for SAB-139 and other Tc-hIgG products.

In addition to directly neutralizing viral fusion and/or entry into host cells, antibodies can contribute to control of infection and clearance of virus through their Fc domain via activation of innate immune cells such as neutrophils, monocytes, and NK cells via phagocytosis of virus and/or antibody-dependent cellular cytotoxicity (ADCC) of infected cells. For example, ADNP is initiated after IgG-immune complex Fc binding to the activating receptor Fcγ-RIIIB [40], which shares the same extracellular domain and therefore similar binding profiles to IgG as Fcγ-RIIIA. In contrast, ADMP is driven through IgG-immunocomplex Fc binding to both the activating receptors Fcγ-RIIA and Fcγ-RIIIA [41]. Thus, differential binding of the SAB-139 IgG antibodies may be related to the differences in Fc-receptors used to drive ADNP and/or ADMP. Natural killer cells only express Fcγ-RIIIA, and, similar to ADNP, activated NK cells degranulate (CD107a expression) [41, 42] and produce cytokines IFN-γ and the chemokine MIP-1β to induce ADCC of infected cells. A growing body of evidence suggests that ADCC may contribute to the efficacy of some monoclonal antibodies against EBOV [43–45], and both NK cells and monocytes have been implicated in protection against EBOV [46, 47] disease in NHP models.

We demonstrate that SAB-139 strongly activated 3 classes of human phagocytic and/or ADCC-effector cells (monocytes, neutrophils, and NK cells) in vitro, indicating that the Fc-domain protein and glycosylation structure of Tc-bovine IgGs are highly functional and strongly interact with FcR-bearing cells [36]. Therefore, SAB-139 should recruit innate immunity effector cells/activity in humans. In addition, the IgG1 subtype, a potent activator of ADCC, comprises 90% of SAB-139 compared with the typical range of 60%–70% in human-derived IVIG products [48]. The ability of IgG1 and/or IgG3 antibodies to induce multiple Fc-domain-mediated effector functions, termed polyfunctionality, has been associated with elite controllers of human immunodeficiency virus-1 infection. This polyfunctionality may have relevance to the efficacy of immunotherapeutics against EBOV and other viral agents [49, 50]. Therefore, SAB-139 may activate more global effector-cell responses in humans than is functionally possible from animal-derived IVIG (non-human Fc regions) or human-derived IVIG (proportionally less IgG1).

The in vivo results indicate that SAB-139/V6–V8, delivered up to 3 d after EBOV exposure, can protect NHPs from death or illness. More importantly, all infused doses of SAB-139 were well tolerated in all NHPs even when the animals were highly viremic. The results also indicate that low-dose, lower-potency SAB-139 (V3–V4) delivered 1 d after EBOV infection or higher dose, higher potency SAB-139 (V6–V8) delivered 5 d after EBOV infection provided limited or no protection. Of note, NHPs from the LI group were already highly viremic and had blood chemistry abnormalities before or at d 5 postinfection. Therefore, EBOV infection was advanced by the time Tc-hIgG therapy was initiated, and most NHPs succumbed within 2 d (d 7 postinfection) after treatment. Better survival may have been obtained had we delivered more of lower potency SAB-139/V3–V4 at d 1 postinfection or higher potency SAB-139/V6–V8 at d 5 postinfection, respectively. Alternatively, a more compressed dosing schedule could be implemented up to and including single administration of the total planned dose on the first d of treatment to improve efficacy. However, although this dosing schedule may be practical in a human patient care scenario, administration of such a volume to sedated NHPs in

a BSL4 setting was not practical due to time or logistical constraints. A study with a smaller group of NHPs could answer this question.

In addition, SAB-139 (and possibly other EBOV immunotherapeutics) delivered early in a primary EBOV infection prevented the development of a protective, adapted immune response. This lack of adapted immune response was indicated by the death of the majority of EI NHPs (5 of 6) but none of the DI NHPs (0 of 4) at back-challenge (Experiment 2, Supplementary Table 8S). Fatalities occurred in the EI group despite the presence of anti-EBOV GP antibodies at back-challenge and a history of transient anti-NP antibodies during the postprimary infection recovery phase. The mechanism(s) preventing adaptive immunity is not known. We conjecture that SAB-139 delivered 1 d, but not 3 d, after infection bound and masked the epitopes of EBOV GP antigen while also stimulating innate-immunity effector cells via Fc receptor binding causing the release of immunomodulating cytokines. This masking then prevented T and/or B cells from developing an adequate protective-adaptive immune response. However, further studies are needed to clarify the mechanism(s) of this observation.

CONCLUSIONS

Taken together, the in vitro and in vivo data suggest that SAB-139 has an acceptable intrinsic-safety profile for human use. SAB-139 was efficacious in neutralizing virus in vitro, strongly induced innate immune effector functions, and protected NHPs from EBOV disease. These results suggest that SAB-139 may be effective in treating human-EBOV infection and could progress into clinical evaluation. As a response platform for new and emerging infectious diseases, the current manufacturing process can produce GMP Tc-hIgGs 75 d after immunization begins with existing or experimental plasmid DNA, recombinant protein, or whole-virus vaccine. Methods to further reduce production time are being considered and investigated. These methods include prepriming the Tc-bovines with vaccines against known pathogens of interest, prime-boost combinations with different vaccines, new adjuvants that increase or accelerate the immune response, and further genetic engineering to improve the adaptive immune response and human-antibody yield. Finally, future in vitro and in vivo studies that compare SAB-139 with other anti-EBOV antibody products in animals and/or humans should be considered.

Supplementary Data

Supplementary materials are available at The Journal of Infectious Diseases online. Consisting of data provided by the authors to benefit the reader, the posted materials are not copyedited and are the sole responsibility of the authors, so questions or comments should be addressed to the corresponding author.

Notes

Author contributions. T. L., R. S. B., D. M. G., L. E. H., G. G. O., E. S., J. D., J. H., G. S., and P. B. J. were responsible for initial study design, although most authors were involved with subsequent study amendments. S. K. conducted the surface plasmon resonance experiments. G. A. conducted the effector cell function experiments. T. B., E. P., and S. M. conducted in vitro neutralizing assessments against EBOV. R. S. B., D. R., M. S., and N. O. performed animal observations and sample collections. K. B. J. coordinated efforts across Core Services and completed glycoprotein and nucleoprotein ELISAs. K. A. B., T. H., and K. F. completed sequencing and bioinformatic analysis. T. L., R. S. B., and D. M. G. reviewed data and developed the manuscript. L. B. and J. W. provided manuscript writing and figure development, respectively. E. S., H. W., and J. J. were responsible for SAB-139 manufacturing and quality control testing.

Acknowledgments. Ebola virus/H.sapiens-tc/GIN/2014/Makona-C05 isolate was generously provided by Dr. Kobinger of Public Health Agency of Canada. Cetuximab was provided as a gift from Dr. John Lee at Sanford Research, Sioux Falls, SD. We thank the dedicated animal care staff for their efforts during the in vivo studies: Prudencia Avila, Tiffany Briggs, Yescenia Varela, Nicholas Vaughan, Isis Alexander, Kurt Cooper, Kristina Howard, Erin Kollins, Rebecca Reeder, Kaleb Sharer, and Lisa Torzewski. We thank Srikanth Yellayi for conducting necropsies and histologic analysis. We also thank the following: Melanie Cohen, Jon Marchand, Justin Varghese, and Sharon Altmann for ELISA testing support; Sylvan McDowell, Jon Marchand, Angela Wenttang, Josh Johnson, Rebecca Shim, Catherine M. Jett, and Ken Jensen for study support; and Ricky Adams and Daniel Ackerman for molecular analysis.

Disclaimer. The views expressed in this article are those of the authors and do not necessarily reflect the official policy of the Departments of Health and Human Services or Defense, the US Army, US Navy, Department of Defense, nor the US Government or other participating organizations. Some of the authors are employees of the US Government. This work was prepared as part of their official duties. Title 17 U.S.C. §105 provides that "Copyright protection under this title is not available for any work of the United States Government." Title 17 U.S.C. §101 defines a US Government work as a work prepared by a military service member or employee of the US Government as part of that person's official duties. The use of trade names, commercial products, or organizations does not imply endorsement by the US Government.

Financial support. Research activities by the federal government laboratories were collaboratively conducted as a result of the National Interagency Confederation for Biological Research. This work was partially funded by the Division of Intramural Research of the National Institute of Allergy and Infectious Diseases (NIAID), Division of Clinical Research, Integrated Research Facility and Battelle Memorial Institute's prime contract with NIAID (contract no. HHSN272200700016I). The NHPs were provided by the Division of Microbiology and Infectious Diseases at NIAID. The study was partly funded by the Naval Medical Research Center, Viral and Rickettsial Diseases Department and Biologic Defense Research Directorate, under contract no. N62645-14-C-4034 and by The Henry Jackson Foundation for the Advancement of Military Medicine contract with the US Navy (contract no. Omnibus III DO-0005). This work is part of a supplement sponsored by SAB Biotherapeutics Inc.

Potential conflicts of interest. The authors declare competing financial interests. Authors from SAB Biotherapeutics, Inc. (HW, JJ, and ES) and Novavax, Inc. (GS and GG) were employees of these for-profit organizations at the time of the study, and authors from these organizations have financial interests in their respective companies. Some authors (JH and ES) submitted pending patent applications that are related to this work (United States Patent Application 15/361279, 25 November 2015). The authors developed a lead candidate therapeutic antibody (SAB-139) from this work, which would be considered a product for further development by SAB as a commercial venture. SAB has an Investigational New Animal Drug (INAD) file with US Food and Drug Administration Center for Veterinary Medicine (no. I-011204) with regard to the complete genetic engineering of the transchromosomic bovine antibodies and data regarding the production of

fully human antibody in the animals. This INDA does not alter the authors' adherence to policies on sharing data and materials. All authors have submitted the ICMJE Form for Disclosure of Potential Conflicts of Interest. Conflicts that the editors consider relevant to the content of the manuscript have been disclosed.

References

1. Luke TC, Casadevall A, Watowich SJ, Hoffman SL, Beigel JH, Burgess TH. Hark back: passive immunotherapy for influenza and other serious infections. Crit Care Med **2010**; 38:e66–73.
2. Luke TC, Kilbane EM, Jackson JL, Hoffman SL. Meta-analysis: convalescent blood products for Spanish influenza pneumonia: a future H5N1 treatment? Ann Intern Med **2006**; 145:599–609.
3. Mair-Jenkins J, Saavedra-Campos M, Baillie JK, et al. The effectiveness of convalescent plasma and hyperimmune immunoglobulin for the treatment of severe acute respiratory infections of viral etiology: a systematic review and exploratory meta-analysis. J Infect Dis **2015**; 211:80–90.
4. Qiu X, Wong G, Audet J, et al. Reversion of advanced Ebola virus disease in nonhuman primates with ZMapp. Nature **2014**; 514:47–53.
5. Dowall SD, Bosworth A, Rayner E, et al. Post-exposure treatment of Ebola virus disease in guinea pigs using EBOTAb, an ovine antibody-based therapeutic. Sci Rep **2016**; 6:30497.
6. Jahrling PB, Geisbert J, Swearengen JR, et al. Passive immunization of Ebola virus-infected cynomolgus monkeys with immunoglobulin from hyperimmune horses. Arch Virol Suppl **1996**; 11:135–40.
7. Platts-Mills TA, Schuyler AJ, Tripathi A, Commins SP. Anaphylaxis to the carbohydrate side chain alpha-gal. Immunol Allergy Clin North Am **2015**; 35:247–60.
8. Sim DW, Lee JS, Park KH, et al. Accurate assessment of alpha-gal syndrome using cetuximab and bovine thyroglobulin-specific IgE. Mol Nutr Food Res **2017**.
9. Sano A, Matsushita H, Wu H, et al. Physiological level production of antigen-specific human immunoglobulin in cloned transchromosomic cattle. PLoS One **2013**; 8:e78119.
10. Matsushita H, Sano A, Wu H, et al. Species-specific chromosome engineering greatly improves fully human polyclonal antibody production profile in cattle. PLoS One **2015**; 10:e0130699.
11. Matsushita H, Sano A, Wu H, et al. Triple immunoglobulin gene knockout transchromosomic cattle: bovine lambda cluster deletion and its effect on fully human polyclonal antibody production. PLoS One **2014**; 9:e90383.
12. Kuroiwa Y, Kasinathan P, Sathiyaseelan T, et al. Antigen-specific human polyclonal antibodies from hyperimmunized cattle. Nat Biotechnol **2009**; 27:173–81.
13. Dye JM, Wu H, Hooper JW, et al. Production of potent fully human polyclonal antibodies against Ebola Zaire virus in transchromosomal cattle. Sci Rep **2016**; 6:24897.
14. Luke T, Wu H, Zhao J, et al. Human polyclonal immunoglobulin G from transchromosomic bovines inhibits MERS-CoV in vivo. Sci Transl Med **2016**; 8:326ra21.
15. Hooper JW, Brocato RL, Kwilas SA, et al. DNA vaccine-derived human IgG produced in transchromosomal bovines protect in lethal models of hantavirus pulmonary syndrome. Sci Transl Med **2014**; 6:264ra162.
16. Bounds CE, Kwilas SA, Kuehne AI, et al. Human polyclonal antibodies produced through DNA vaccination of transchromosomal cattle provide mice with post-exposure protection against lethal Zaire and Sudan Ebolaviruses. PLoS One **2015**; 10:e0137786.
17. Arabi YM, Balkhy HH, Hayden FG, et al. Middle East respiratory syndrome. N Engl J Med **2017**; 376:584–94.
18. Beigel JH, Voell J, Kumar P, et al. Safety and tolerability of a novel, polyclonal human anti-MERS coronavirus antibody produced from transchromosomic cattle: a phase 1 randomised, double-blind, single-dose-escalation study. Lancet Infect Dis **2018**; 18:410–8.
19. Silver JN, Ashbaugh CD, Miles JJ, et al. Deployment of transchromosoma bovine for personalized antimicrobial therapy. Clin Infect Dis **2018**; 66:1116–9.
20. Gilman JK, Wright M, Clifford Lane H, Schoomaker EB. A model of federal interagency cooperation: the National Interagency Confederation for Biological Research. Biosecur Bioterror **2014**; 12:144–50.
21. Hahn TJ, Webb B, Kutney J, et al. Rapid manufacture and release of a GMP batch of Zaire ebolavirus glycoprotein vaccine made using recombinant baculovirus-Sf9 insect cell culture technology. J Bioprocess **2015**; 14:6–14.
22. Hoenen T, Groseth A, Feldmann F, et al. Complete genome sequences of three Ebola virus isolates from the 2014 outbreak in west Africa. Genome Announc **2014**; 2: pii: e01331-14.
23. Honko AN, Johnson JC, Marchand JS, et al. High dose sertraline monotherapy fails to protect rhesus macaques from lethal challenge with Ebola virus Makona. Sci Rep **2017**; 7:5886.
24. Trefry JC, Wollen SE, Nasar F, et al. Ebola virus infections in nonhuman primates are temporally influenced by glycoprotein poly-U editing site populations in the exposure material. Viruses **2015**; 7:6739–54.
25. Regules JA, Beigel JH, Paolino KM, et al. A recombinant vesicular stomatitis virus Ebola vaccine. N Engl J Med **2017**; 376:330–41.
26. Rimoin AW, Lu K, Bramble MS, et al. Ebola virus neutralizing antibodies detectable in survivors of theYambuku, Zaire outbreak 40 years after infection. J Infect Dis **2018**; 217:223–31.
27. Bowen ET, Baskerville A, Cantell K, Mann GF, Simpson DI, Zuckerman AJ. The effect of interferon on experimental Ebola virus infection in rhesus monkeys. In: Pattyn S, ed. Ebola Virus Haemorrhagic Fever. Amsterdam: Elsevier/North Holland, **1978**: pp 167–71.
28. Johnson RF, Hammoud DA, Lackemeyer MG, et al. Small particle aerosol inoculation of cowpox Brighton Red in rhesus monkeys results in a severe respiratory disease. Virology **2015**; 481:124–35.
29. Mate SE, Kugelman JR, Nyenswah TG, et al. Molecular evidence of sexual transmission of Ebola virus. N Engl J Med **2015**; 373:2448–54.
30. Kugelman JR, Wiley MR, Mate S, et al. Monitoring of Ebola virus Makona evolution through establishment of advanced genomic capability in Liberia. Emerg Infect Dis **2015**; 21:1135–43.
31. R Core Team. The R project for statistical computing. Available at: https://www.r-project.org/. Accessed January 26, 2018.
32. Hiatt A, Pauly M, Whaley K, Qiu X, Kobinger G, Zeitlin L. The emergence of antibody therapies for Ebola. Hum Antibodies **2015**; 23:49–56.
33. Oswald WB, Geisbert TW, Davis KJ, et al. Neutralizing antibody fails to impact the course of Ebola virus infection in monkeys. PLoS Pathog **2007**; 3:e9.
34. Huang Y, Ferrari G, Alter G, et al. Diversity of antiviral IgG effector activities observed in HIV-infected and vaccinated subjects. J Immunol **2016**; 197:4603–12.
35. Brown EP, Licht AF, Dugast AS, et al. High-throughput, multiplexed IgG subclassing of antigen-specific antibodies from clinical samples. J Immunol Methods **2012**; 386:117–23.
36. Borrok MJ, Jung ST, Kang TH, Monzingo AF, Georgiou G. Revisiting the role of glycosylation in the structure of human IgG Fc. ACS Chem Biol **2012**; 7:1596–602.
37. Hogarth PM. Fc receptors: introduction. Immunol Rev **2015**; 268:1–5.
38. Bournazos S, Ravetch JV. Diversification of IgG effector functions. Int Immunol **2017**; 29:303–10.
39. Fischer J, Eberlein B, Hilger C, et al. Alpha-gal is a possible target of IgE-mediated reactivity to antivenom. Allergy **2017**; 72:764–71.
40. Lassaunière R, Musekiwa A, Gray GE, Kuhn L, Tiemessen CT. Perinatal HIV-1 transmission: Fc gamma receptor variability associates with maternal infectiousness and infant susceptibility. Retrovirology **2016**; 13:40.
41. Moldt B, Schultz N, Dunlop DC, et al. A panel of IgG1 b12 variants with selectively diminished or enhanced affinity for Fcγ receptors to define the role of effector functions in protection against HIV. J Virol **2011**; 85:10572–81.
42. Chung AW, Rollman E, Center RJ, Kent SJ, Stratov I. Rapid degranulation of NK cells following activation by HIV-specific antibodies. J Immunol **2009**; 182:1202–10.
43. Corti D, Misasi J, Mulangu S, et al. Protective monotherapy against lethal Ebola virus infection by a potently neutralizing antibody. Science **2016**; 351:1339–42.
44. Liu Q, Fan C, Li Q, et al. Antibody-dependent-cellular-cytotoxicity-inducing antibodies significantly affect the post-exposure treatment of Ebola virus infection. Sci Rep **2017**; 7:45552.
45. Zeitlin L, Pettitt J, Scully C, et al. Enhanced potency of a fucose-free monoclonal antibody being developed as an Ebola virus immunoprotectant. Proc Natl Acad Sci U S A **2011**; 108:20690–4.
46. Warfield KL, Perkins JG, Swenson DL, et al. Role of natural killer cells in innate protection against lethal ebola virus infection. J Exp Med **2004**; 200:169–79.
47. Lüdtke A, Ruibal P, Becker-Ziaja B, et al. Ebola virus disease is characterized by poor activation and reduced levels of circulating CD16+ monocytes. J Infect Dis **2016**; 214:275–80.
48. Smith B. Concepts in Immunology and Immunotherapeutics. 4th ed. Bethesda, MD: American Society of Health-Systems Pharmacists, **2008**.
49. Ackerman ME, Mikhailova A, Brown EP, et al. Polyfunctional HIV-specific antibody responses are associated with spontaneous HIV control. PLoS Pathog **2016**; 12:e1005315.
50. Schmaljohn A, Lewis GK. Cell-targeting antibodies in immunity to Ebola. Pathog Dis **2016**; 74:ftw021.